Earth and Planetary Science Letters 270 (2008) 209–220

Contents lists available at ScienceDirect

Earth and Planetary Science Letters

journal homepage: www.elsevier.com/locate/epsl

Detecting co-seismic displacements in glaciated regions: An example from the great November 2002 Denali earthquake using SPOT horizontal offsets

Michael H. Taylor [a,*], Sebastien Leprince [b], Jean-Philippe Avouac [b], Kerry Sieh [b]

[a] Departmernt of Geology, University of Kansas, 120-Lindley Hall, Lawrence, Kansas 66045, United States
[b] California Institute of Technology, Division of Geological and Planetary Sciences, Pasadena, CA, 91125, United States

ARTICLE INFO

Article history:
Received 14 September 2007
Received in revised form 27 February 2008
Accepted 9 March 2008
Available online 25 March 2008

Editor: R.D. van der Hilst

Keywords:
Alaska
Denali earthquake
earthquake rupture
SPOT offsets

ABSTRACT

We use SPOT image pairs to determine horizontal offsets associated with the Mw 7.9 November 2002 Denali earthquake in the vicinity of Slate Creek, AK. Field measurements and aerial photographs are used to further characterize the geometry of the surface rupture. Aerial photographs show that shear localization occurs where the rupture trace is linear, and distributed off-fault deformation is common at fault bends and step-overs, or at geologic contacts between rock, glacial sediments, and ice. The displacement field is generated using a sub-pixel cross correlation technique between SPOT images taken before and after the earthquake. We identify the effects of glacier motion in order to isolate the tectonic displacements associated with the Denali earthquake. The resulting horizontal displacement field shows an along-strike variation in dextral shear, with a maximum of approximately 7.5 m in the east near 144° 52′W, which decreases to about 5 m to the west near 145° 45′W. If the November 2002 earthquake represents the long-term behavior of the Denali fault, it implies a westward decrease in the long-term dextral slip rate. A possible mechanism to accommodate the westward decreasing slip on the Denali fault is to transfer fault slip to adjacent east-trending contractional structures in the western region of the central Alaskan Range.

Published by Elsevier B.V.

1. Introduction

Field observations are critical to understand the details of earthquake rupture and the magnitude of co-seismic slip generated by great earthquakes. These observations may shed light into the dynamics of earthquake rupture (Poliakov et al., 2002) and the constitutive properties of fault zones (Wald and Heaton, 1994; Fialko, 2004). However, robust field measurements are only possible where clear offset features can be identified. For example, ideal piercing points such as offset thalwegs and risers between river terraces should be linear and oriented perpendicular to the fault zone to obtain an accurate and precise measurement of the horizontal and vertical components of co-seismic slip. Otherwise, a general caveat is that the knowledge of the pre-existing geometry for the offset feature is implied. In addition, if the aperture of co-seismic slip is distributed over a wide zone of several hundred meters or more, one cannot rule out the possibility that a significant portion of the slip distribution may escape detection (e.g., McGill and Rubin, 1999). Space-borne geodesy such as Synthetic Aperture Radar Interferometry (InSAR), while highly accurate in measuring the line of sight displacement, is commonly unable to resolve the complexities associated with the near-field region of co-seismic displacement (Michel et al., 1999). This is due in large part to high near-field strain generated during large earthquakes, which results in saturation of the near-field phase signal (Michel et al., 1999; Simons et al., 2002), and a loss of coherence may also occur due to intense ground shaking. However, sub-pixel correlation of SAR amplitude images can partially account for the north–south and east–west components of the surface displacement field (Elliott et al., 2007). Additionally, confidence in resolving the three dimensional displacement field is reliant on independent displacement measurements and model constraints. Geodetic measurements using the Global Positioning System (GPS) are also unable to precisely resolve the details of the near-field co-seismic displacement. The main limitation with GPS is that it lacks the necessary spatial resolution.

During November 3, 2002 a thrust earthquake occurred on the previously unknown south-directed Susitna Glacier thrust fault (Eberhart-Phillips et al., 2003; Haeussler et al., 2004). This sub-event triggered dextral slip sub-events on the Denali fault, which culminated in the great Mw 7.9 earthquake; the largest continental strike–slip earthquake at the time, to be documented both instrumentally and in the field. As a result, the 2002 Denali earthquake's rupture geometry and co-seismic slip distribution is one of the most robustly documented strike–slip events (Haeussler et al., 2004). In this paper we obtain estimates of the horizontal co-seismic displacement field along the eastern segment of the 2002 rupture from 10 m panchromatic SPOT imagery. Our analysis occurs near the region of highest documented co-seismic slip, and provides an opportunity to make a

* Corresponding author. Tel.: +1 785 864 5828; fax: +1 785 864 5276.
E-mail address: mht@ku.edu (M.H. Taylor).

0012-821X/$ – see front matter. Published by Elsevier B.V.
doi:10.1016/j.epsl.2008.03.028

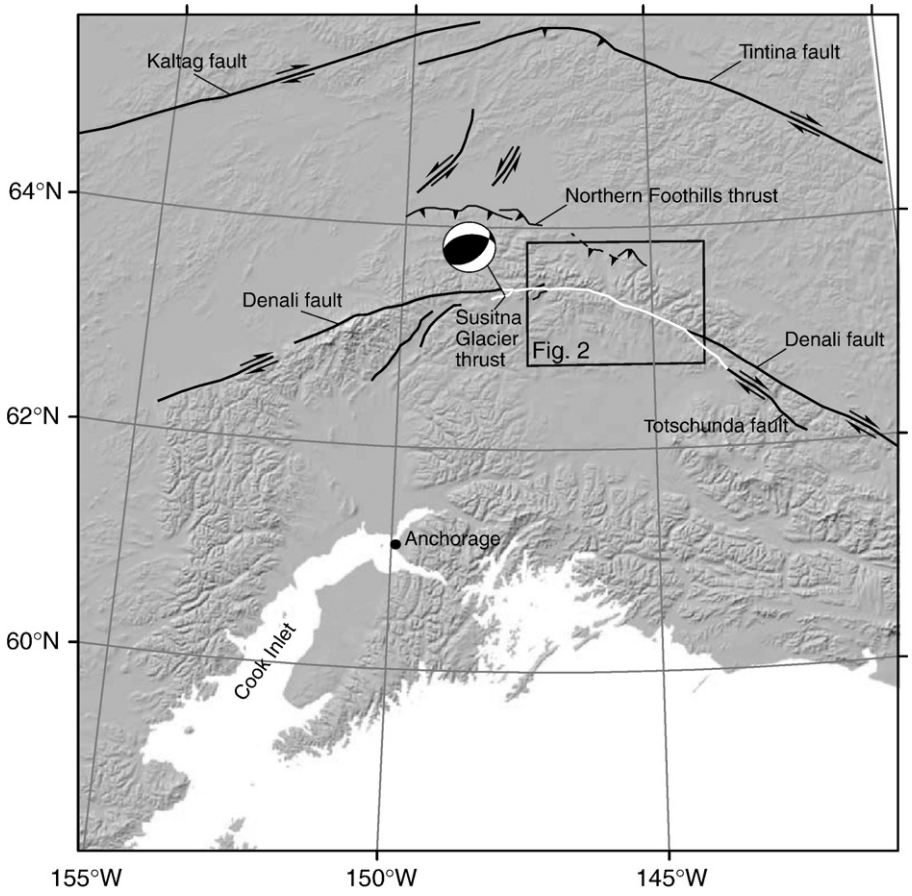

Fig. 1. Shaded grayscale image of south and central Alaska generated from GTOPO30, showing distribution of significant arcuate strike slip faults and related thrust faults and extent of the December 2002 rupture in white. Arrows indicate strike–slip motion; barbs are on the hanging wall of thrust faults; SGT-Susitna Glacier Thrust.

comparative study with previous field and geodetic measurements. In this study, we have identified anomalous horizontal motions related to glacier flow that can significantly swamp the co-seismic signal in optical images. To mitigate the effects of glacial motions, we have developed a technique to identify and remove them, and isolate the co-seismic slip of the 2002 Denali earthquake.

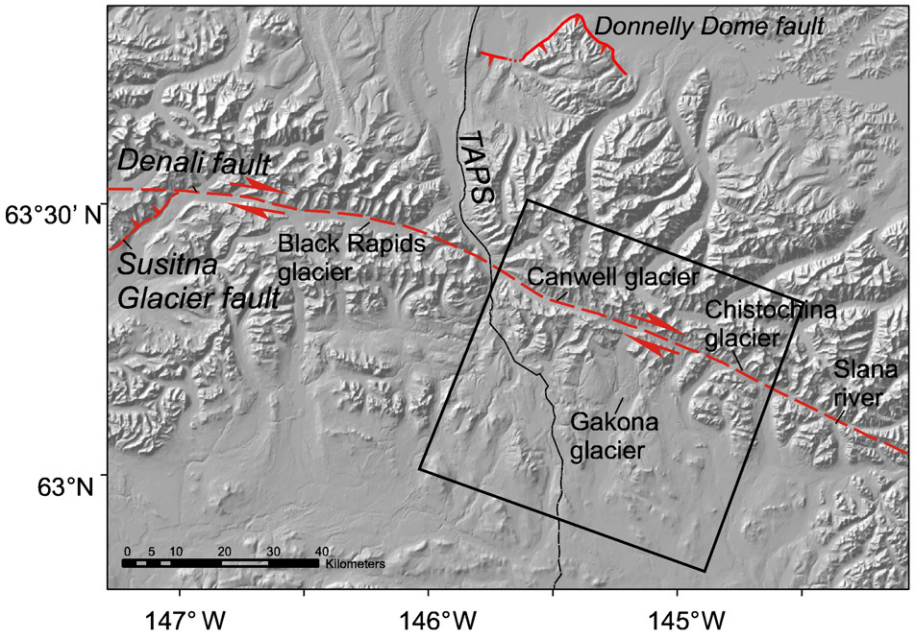

Fig. 2. Shaded relief map generated from the NED DEM. Illumination is from azimuth 315°. The Denali fault strikes ~N60°W in the east, and changes to an approximate east–west strike to the west. Note the distribution of north and south flowing glaciers. Box indicates location of Fig. 7. Thrust faults are indicated with barbs on the hanging wall and strike–slip faults are indicated by arrows. TAPS=Trans Alaskan Pipeline. See Fig. 1 for location.

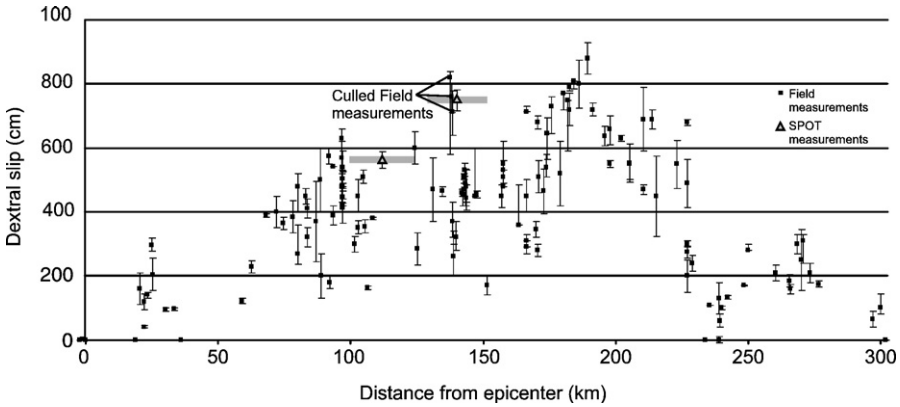

Fig. 3. A compilation of field measurements plotted as magnitude of dextral slip as a function of distance along the entire 2002 rupture, and includes the Susitna Glacier, Denali, and Toschunda fault segments (Haeussler et al., 2004). For details of field measurements, associated uncertainties, and collection dates, please see Haeussler et al. (2004). Estimates of co-seismic slip determined from SPOT horizontal offsets are plotted in comparison as grey triangles and data swaths are represented by horizontal gray bars. See text for a detailed discussion and Fig. 8 for profile locations for the SPOT measurements.

In the following sections, we first provide a brief overview of the regional tectonics of the Alaska Range and the 2002 Denali earthquake. We then follow with an overview of the field measurements of the rupture made by numerous workers (Eberhart-Phillips et al., 2003; Haeussler et al., 2004), and our own field observations. Aerial photographs provide additional details associated with the rupture geometry. This is followed by the processing methodology and data processing challenges due to snow and ice effects to obtain the horizontal offsets from the SPOT images (Van Puymbroeck et al., 2000; LePrince et al., 2007). We then compare the SPOT horizontal offsets with the field measurements and aerial photographs. Collectively, our results allow us to assess the observed surface displacements, and separate glacier movements from the co-seismic fault slip generated by the 2002 Denali earthquake.

2. Tectonic framework of the Alaska Range

Although the principal element of the North American-Pacific plate boundary is the Alaska–Aleutian megathrust, an array of interacting fault systems comprised of strike–slip and thrust faults occur within the upper plate of the plate boundary zone. The Alaska Range is a significant tectonic element of the plate boundary and is an east-trending arcuate orogenic belt within central Alaska (Fig. 1). Traversing the rugged Alaska Range is the arcuate right-slip Denali fault, which in 2002 experienced an earthquake sequence triggered by the south-directed Susitna Glacier thrust, culminating in a Mw 7.9 sub-event on the Denali (Eberhart-Phillips et al., 2003). At the time, this was the largest continental strike–slip event to be recorded by modern instrumentation. Initiation of the Denali fault is estimated to be Late Cretaceous (Nokelberg et al., 1985), and the magnitude of right-slip displacement along the Denali fault ranges from 350–400 km along its eastern segment, to ~32 km on the McKinley strand to the west based on offset lithologic units (Eisbacher, 1976; Hickman et al., 1977; Jones et al., 1982; Plafker et al., 1989; Nokelberg et al., 1992; Plafker and Berg, 1994).

To the north of the Denali fault, the structural style and lithologic units of the Alaska Range records the progressive accretion of island arc assemblages onto the former continental margin of North America beginning in the Late Jurassic (Ridgeway et al., 2002). Reactivation of the suture zones and development of the north-directed fold-thrust belt is recorded in sediments of the upper Cretaceous Cantwell basin that has been regionally shortened (Fig. 1) (Pewe et al., 1966; Wahrhaftig, 1970a,b,c; Csejtey et al., 1992; Cole et al., 1999; Ridgeway et al., 2002). Transpression along the Denali fault has resulted in recent uplift of the eastern and central Alaska Range as recorded by Late Eocene to Holocene conglomerates within the Tanana Basin to the north (Fig. 1). North-directed thrust faulting is apparently active to the north of the Denali, as indicated by Paleozoic strata thrust over Pliocene to Quaternary sediments in the vicinity of the Delta River along the Donnelly Dome fault (Fig. 2) (Ridgeway et al., 2002).

Besides the initial geomorphic and geologic studies conducted by Wahrhaftig (Wahrhaftig, 1958, 1968; Wahrhaftig et al., 1969; Wahrhaftig, 1970a,b,c,d,e,f,g,h; Wahrhaftig et al., 1975; Wahrhaftig, 1987), the active tectonics along the northern margin of the Alaska Range is in large part unexplored. In particular, a quantitative estimate of the shortening rate over Quaternary time is unknown. Recently, reconnaissance studies (Bemis, 2004) indicate that the northern foothills of the Alaska Range are bounded by an active-to-recently-active north-directed fold-thrust belt. In more detail, the topography of the Alaska Range and the northern foothills indicates that the N–S width of the fold-thrust belt is asymmetric and increases from ~30 km in the east, to over 60 km to the west (Fig. 1). The regions of highest elevation are generally confined to the north of the Denali fault near its apex, and to the south of the fault in the Mt. McKinley area (Fig. 1).

3. Denali 2002 earthquake

The Mw 7.9 November 3, 2002 Denali earthquake ruptured three interconnected faults, nucleating on the previously unidentified NNW-dipping Susitna Glacier thrust fault located near the apex of the Denali fault (Eberhart-Phillips et al., 2003). The rupture then continued to the east and at the eastern termination of the rupture on the Denali fault, dextral slip was transferred onto the Toschunda fault strand near Mentasta Pass (Fig. 1) (Eberhart-Phillips et al., 2003; Haeussler et al., 2004). The total rupture length is ~341 km, with 218 km of the rupture occurring on the Denali fault (Eberhart-Phillips et al., 2003). The 2002 rupture was subsequently mapped in great detail and numerous co-seismic geomorphic features include mole tracks, pressure ridges, offset terrace risers, en echelon cracks, and Reidel shears observed in snow, ice, and unconsolidated sediments (e.g., Figs. 3–6) (Eberhart-Phillips et al., 2003; Haeussler et al., 2004). Field measurements suggest a markedly asymmetric horizontal slip distribution with 1–3 m of dextral slip occurring in the west, increasing to a maximum of 9 m near the eastern extent of the rupture along the Denali fault (Fig. 3). In comparison for the Toschunda fault, the rupture was essentially symmetric with a maximum dextral displacement of ~2 m at the center of the rupture, falling to zero at the fault tips (Fig. 3) (Eberhart-Phillips et al., 2003; Haeussler et al., 2004). Vertical co-seismic displacements along the Denali rupture were found to be much less than the horizontal slip component. Maximum vertical co-seismic displacements of 1.5 m occurred near km's 105, 175, and 230 of the rupture (see Fig. 10 of Haeussler et al., 2004).

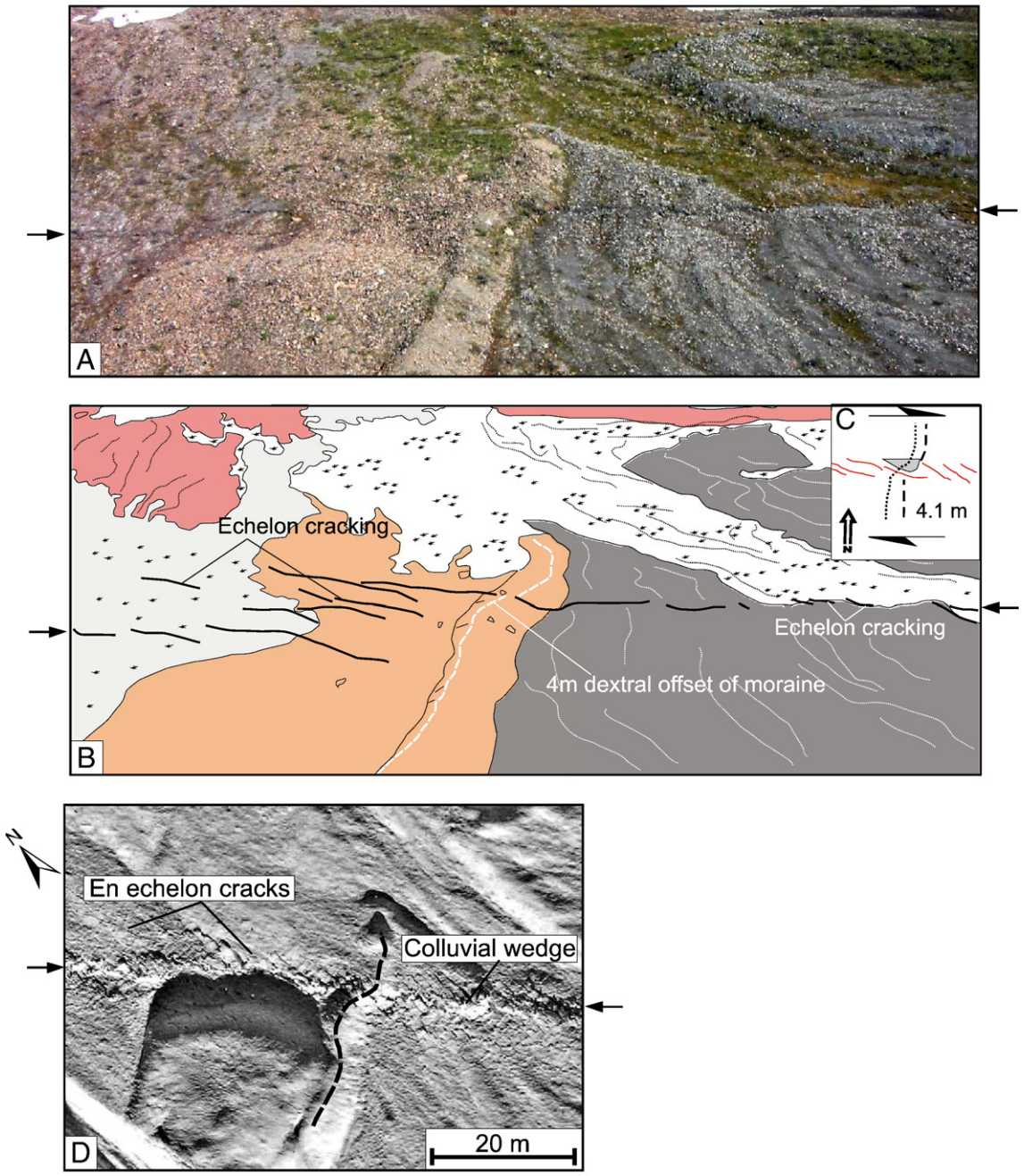

Fig. 4. (A) View to the northeast of a dextrally offset moraine. (B) Sketch of the field relationships observed in (A). (C) Schematic diagram illustrating field relationships observed in (A and B). Dotted line is the location of the moraine crest and the dashed line is the moraine base. Shaded gray area is colluvial wedge related to north-side-up displacement. Note en echelon cracking consistent with dextral shear. (D) Aerial photograph of dextrally offset moraine. Note normal drag consistent with dextral shear, colluvial wedge, and extensive cracking. See Fig. 7 for location, and text for a detailed discussion.

In a study using an inversion of GPS data, the slip function of the Denali 2002 earthquake was also determined to be decidedly asymmetric (Hreinsdottir et al., 2003). Similar to the field observations, the GPS-based model suggests that dextral slip increased from 1–3 m in the west to values of dextral slip exceeding 9 m to the east. The main limitation of this model lies in its inability to resolve any slip along the Susitna Glacier thrust or Toschunda fault segments (Hreinsdottir et al., 2003). A more refined model is presented in a subsequent study with a higher density of GPS measurements to resolve this model limitation (Hreinsdottir et al., 2006). In the following sections, we briefly review the field observations from Haeussler et al. (2004) and present our own observations from Slate Creek and complement these observations with aerial photographs of the rupture obtained on November 11, 2002.

4. Field observations near Slate Creek

The 2002 Denali earthquake ruptured for a total distance of ~341 km, with 218 km of the rupture breaking along the main trace of the Denali fault (Haeussler et al., 2004). We limit our discussion to the region located to the east of the Trans Alaskan Pipeline (TAPS) where the SPOT images cover the Denali fault in the vicinity of the Canwell and Chistochina glaciers (Fig. 2). For a detailed study of field observations made along the entire rupture the reader is directed to

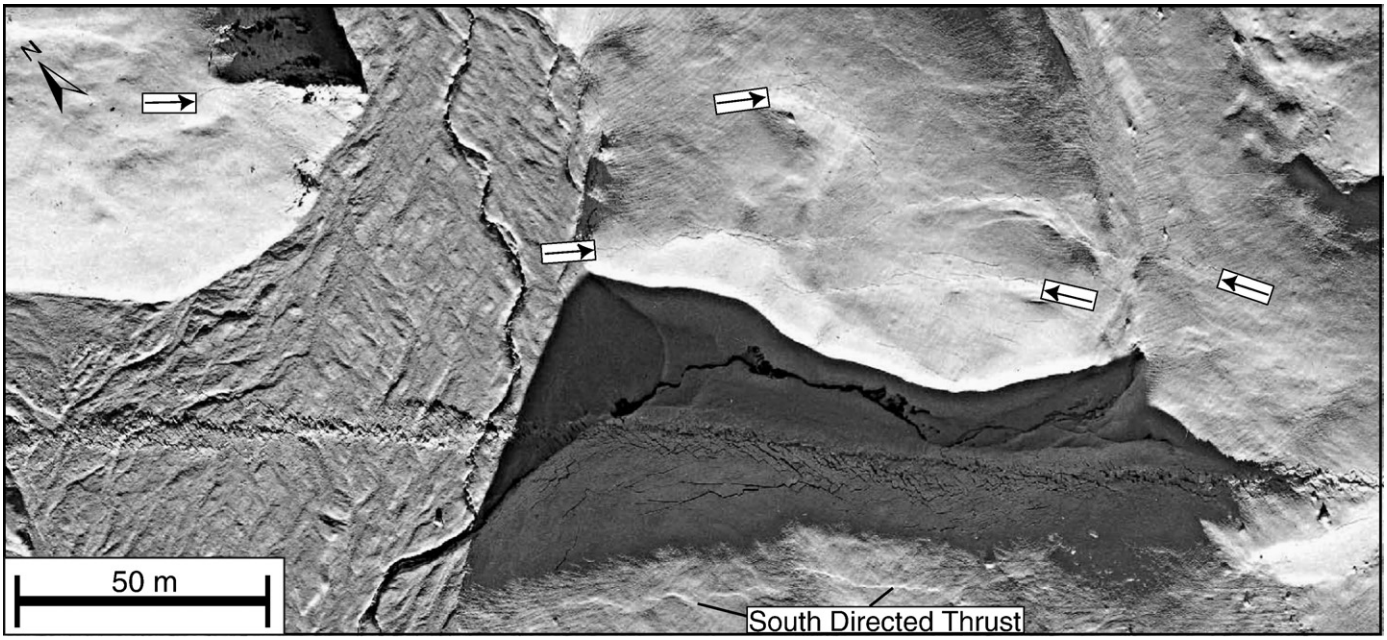

Fig. 5. Air photo of 2002 rupture trace at Slate Creek. Note rupture linearity and shear localization along main trace of the Denali fault, and en echelon cracking, Reidel shears, and cracks associated with ground shaking (black arrows). See text for detailed discussion and Fig. 7 for location.

Haeussler et al. (2004). The segment of the 2002 rupture located east of the TAPS and to the west of the Chistochina glacier is referred to as the 5-meter section (Haeussler et al., 2004). Field observations of dextrally offset features along the western segment near Augustana Creek and eastward to the Delta River range between 3.2 and 5.0 m (eleven measurements) (Fig. 3). From the Delta River in the west to the toe of the Canwell glacier in the east, dextral offsets consistently range between 5.7 and 5.8 m (Haeussler et al., 2004). In general, the rupture is localized and reoccupies fault scarps associated with the main trace of the Denali fault. Commonly, the rupture trace is defined by 2–4 m wide mole tracks comprised of en echelon cracks with orientations consistent with dextral slip. To the east of the Canwell glacier, the rupture crosses glacial ice for 39 km and also crosses the Chistochina glacier for about 5 km (Haeussler et al., 2004). The highest dextral offset mapped in the field along the eastern segment of the '5-meter' section is 6.5 m near Slana Creek (km 174.2 of the rupture) (Haeussler et al., 2004). Interestingly, four field measurements along km's 100–160 are in agreement with the offsets we determined using the SPOT sub-pixel correlation (which we present in Section 7) but were deemed unreliable (Haeussler et al., 2004) (Fig. 3).

Fig. 4 is a field photograph of a dextrally offset moraine located about 1.5 km to the west of the Chistochina glacier. The 2002 rupture crosses the middle of the photo and is defined by a 4 m wide zone of en echelon cracking with crack orientations consistent with dextral slip. The crest of the moraine is comprised of buff colored pebbles and cobbles that range in size from 1–10 cm (Fig. 4). The base of the moraine shows a significant color contrast from the moraine crest, as defined by the dark grey-to-black pebbles and sand (Fig. 4). The rupture does not truncate the moraine crest abruptly, but rather, shows normal drag associated with dextral shear. The crest and base of the moraine are dextrally offset by 4.1 m with an uncertainty of ±20 cm being due to the width of the moraine crest. On the north side of the rupture, we observed five en echelon cracks about 2 m to the east of the moraine crest. Because each crack shows 1–3 cm of opening, the offset estimate should be increased by ~15 cm. We also observed a minor amount of vertical throw for the cracks. A colluvial wedge overlaps the main rupture trace and based on our own field observations, it is related to a north-side up displacement with a vertical component of 0.5 m. The field observations from Haeussler et al. (2004), and our own field measurements indicate that co-seismic displacements associated with the November 2002 earthquake are dominantly dextral with horizontal dextral slip increasing from 3–4 m in the west, to a maximum of 6.5 m in the east.

5. Deformation revealed from aerial photographs

On November 11, 2002 Aeromap U.S. Inc. acquired aerial photographs of the November 2002 rupture to characterize the details of the rupture geometry. Figs. 4D, 5, and 6 show aerial photographs taken in the vicinity of the Chistochina glacier at Slate Creek. The 2002 rupture is particularly clear at this site and in general, reoccupies the main fault zone as indicated by nearby fault scarps related to the main trace of the Denali fault (Figs. 4D, 5). The rupture trace is relatively linear and cuts at a high angle across a series of fluvial terraces and moraines related to south flowing streams and glaciers. The fault zone is narrow, and the rupture is defined by a mole track and associated en echelon cracks that form an approximately 4 m wide rupture on average that is consistent with 4±1 m of dextral slip (Fig. 4D). Off-fault deformation is limited to cracks that are likely related to ground shaking, but we note the cracks reoccupy cumulative fault scarps (Fig. 5). It is also clear from the aerial photograph that a south-directed contractional structure cuts the surface, and field observations indicate it is a south-directed thrust fault (Fig. 5).

Where the surface break approaches the Chistochina glacier from the west, the rupture is abruptly deflected clockwise from the dominant rupture trend by approximately 25° (Fig. 6). Off fault deformation occurs over a zone that is approximately 450 m wide where the rupture abruptly changes its orientation. The deformation zone to the north of the Denali fault occurs directly north of the Chistochina glacier and is comprised of cracks that strike between 090° and 135°. Locally to the south of the rupture, off fault deformation occurs over a 150 m wide zone on the surface of the Chistochina glacier (Fig. 6). The cracks are limited in their extent of the main rupture and have highly variable orientations (Fig. 6). We suggest that cracking related to glacier flow is unlikely, as the cracks only occur adjacent to the rupture, and outside of this zone, the glacier

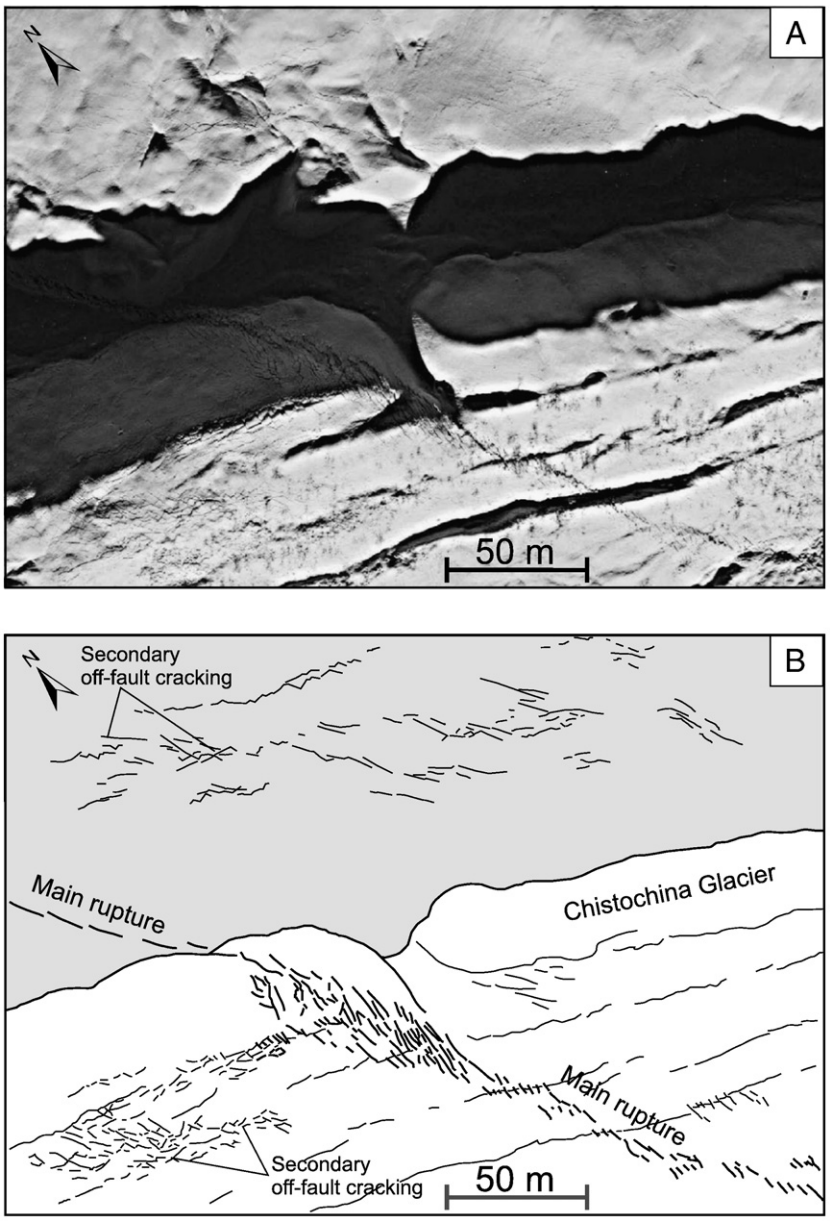

Fig. 6. Air photo of 2002 rupture trace at the Chistochina glacier located just east of Fig. 5. The rupture makes a sharp turn to the south at this site. Note distributed nature of cracking off of the main rupture trace. Cracking associated with glacier flow is unlikely due to the smooth and undisturbed glacier surface in the east part of the Figure. See text for detailed discussion and Fig. 7 for location.

surface is relatively smooth, as shown in Fig. 6 when comparing the west and east sides of the aerial photograph. The distribution of off-fault cracking implies that deformation becomes distributed over larger areas where the rupture geometry either becomes more complex at material boundaries (e.g., the contact between rock and glacial ice or soft glacial sediments) (Hreinsdottir et al., 2006), or at fault bends and step-overs. Deformation tends to be more localized where the fault trace is linear and traverses across more homogeneous material (e.g., Fig. 5).

The fact that deformation observed in the aerial photographs can be well localized on a single rupture in one area and distributed over a fault zone of finite width at another, may provide an explanation for the lateral variation of surface slip as revealed by field measurements. This suggests that the largest field measurements are most representative of fault slip at depth (see discussion in Elliott et al., 2007). Because estimating the magnitude of fault slip at fault complexities from piercing points alone can be difficult, we use the sub-pixel correlation of SPOT optical images. In the following sections we begin with an overview of the sub-pixel correlation technique followed by a new technique for removing the effects of snow cover and active glacier flow, in order to isolate the co-seismic slip of the Denali 2002 earthquake. Like SAR azimuth and range offsets, this technique allows us to map distributed co-seismic strain over a fault zone of finite width, which is difficult to accomplish with field measurements alone.

6. Data analysis: sub-pixel correlation of SPOT optical images

We estimate the horizontal surface deformation associated with the 2002 Denali earthquake using a sub-pixel correlation technique applied to SPOT optical imagery (Van Puymbroeck et al., 2000; LePrince et al., 2007) using the free software package COSI-Corr (Co-Registration of Optically Sensed Images and Correlation) developed at the California Institute of Technology (http://www.tectonics.caltech.edu/slip_history/spot_coseis/).

In this study, we use 10 m panchromatic SPOT 4 images obtained ~10 km east of the Richardson highway that covers the Denali fault

(Fig. 2). Additional image pairs covering this section of the fault that include the 2002 earthquake, and image pairs located to the east and west, with a good chance of retaining coherence, unfortunately did not exist in the SPOT data archive. We use an image pair with a time span of 1.79 yr (656 days, 03/09/2002–20/06/2004, day/month/year) that captures the co-seismic and initial post-seismic phases of the 2002 Denali earthquake (Fig. 7). The images have a near vertical incidence angle (−7° and 7° from vertical). For this technique of tracking horizontal displacements we use a DEM with a resolution much less than the images and 14° of separation between the satellite orbits will unfortunately leave some residual topographic artifacts. We correct for the parallax effects by precise wrapping of the images through the sub-pixel correlation technique. Any stereoscopic effect thus becomes negligible compared to the ground deformation that we measure. The raw images are first coarsely resampled into the same UTM projection using the 40 m resolution NED digital elevation model (DEM) of Alaska. Errors in the satellite orbits (e.g., roll, pitch, and yaw) are corrected during the initial processing using the ephemeris information provided by SPOT Image Corp. The image projection is refined by performing a correlation with a shaded relief image, generated from the NED DEM and the calculated position of the sun during acquisition of the SPOT images. The first raw image is precisely wrapped onto the 40 m resolution NED DEM using accurate sub-pixel Ground Control Points (GCP's). The GCP's are automatically generated following the procedure described in LePrince et al. (2007). The second raw image is then accurately wrapped onto the first orthorectified image using the same procedure. We note that the distribution of snow and ice in the northern part of the image prevented us from having sufficient coverage of GCP's between the two images to the north of the Denali fault and we compensate for this possible lack in registration by using more points to the south of the fault. Once the SPOT images are orthorectified, residual horizontal offsets between the images are quantified by performing a sub-pixel cross-correlation technique, which estimates the slope of the Fourier transform's phase difference for a 32×32 pixel sliding window with an 8 pixel sliding step. The sub-pixel correlation calculates the east–west, and north–south components of the surface horizontal displacement field with an accuracy of 1/20 of a pixel. The signal to noise ratio (SNR) is determined for each image pixel for the corresponding surface displacement. Correlation results with low SNR and those that may also have correspondingly large displacements greater than the largest glacier displacement (>150 m) are masked during post-processing. This removes most data outliers. The spatial sampling used in the cross-correlation determines the final resolution of the surface displacement map. We obtain a surface displacement measurement every 80 m×80 m.

Fig. 8A and B is the surface horizontal displacement maps generated using the sub-pixel correlation technique described

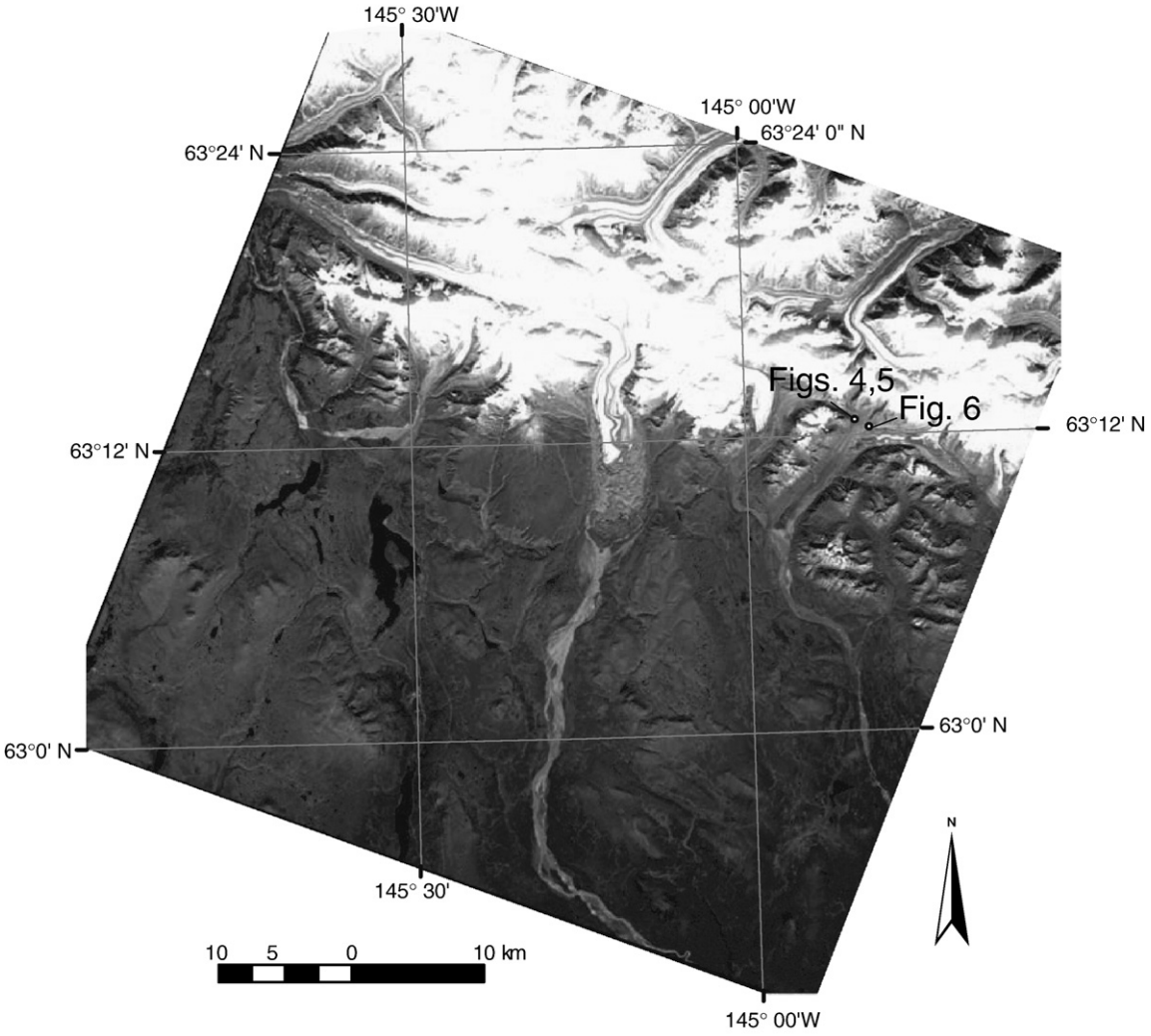

Fig. 7. An example of a SPOT 4 image used to generate the horizontal offset surface displacement field. Note the distribution of snow and glaciers in the vicinity of the Denali fault. The instrument was saturated (white patches) in the vicinity of Denali fault. Locally, patches of bedrock and alluvial fans are represented by lower DN values (i.e., gray regions). Saturated regions with low SNR values were masked during the processing. See Fig. 2 for location.

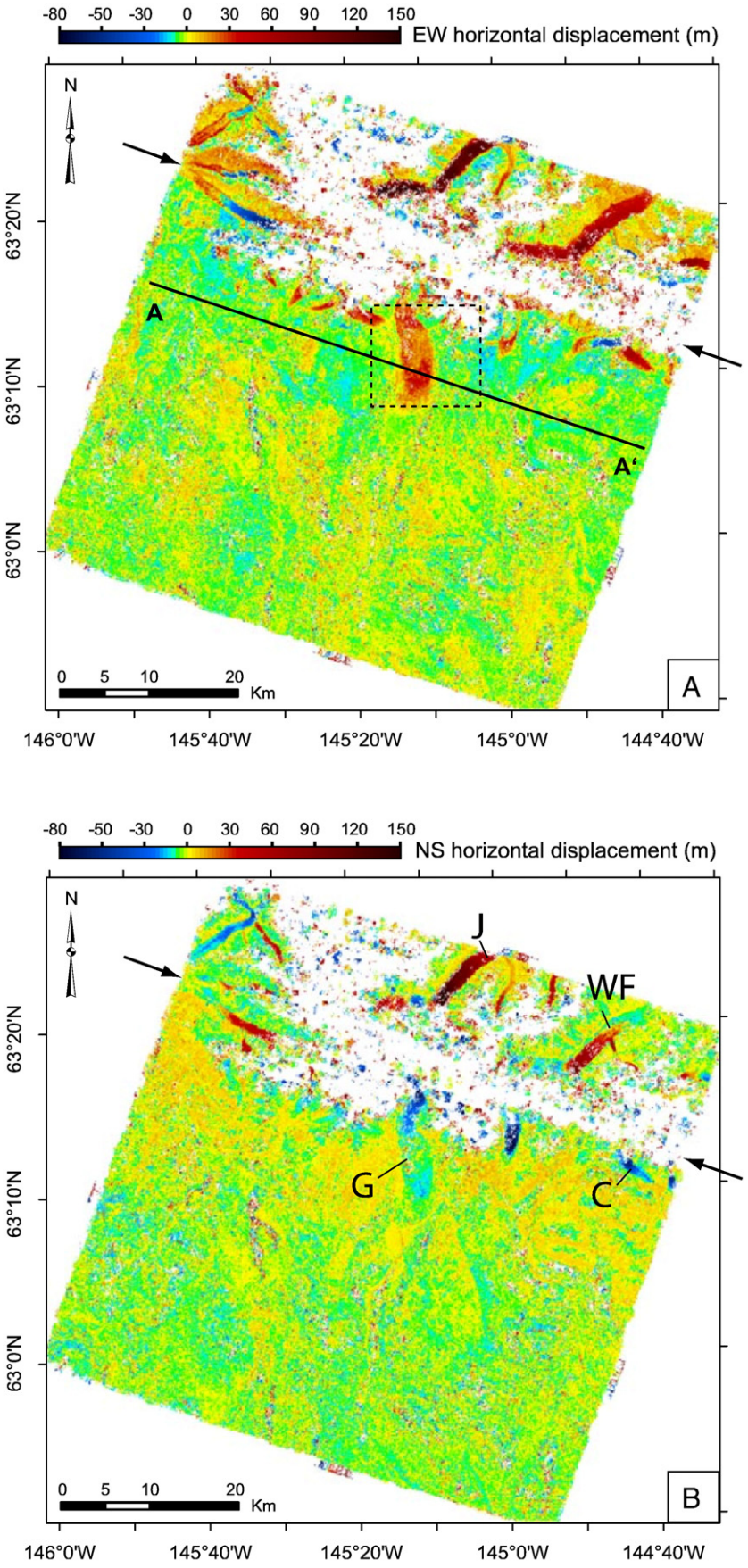

Fig. 8. Maps of the horizontal offset surface displacement field with masked regions in white. We use the convention where eastward and northward displacements are positive. Areas with a low SNR were masked in the processing. Arrows indicate location of the Denali fault. J—Johnson Glacier, WF—West Fork Glacier, C—Chistochina Glacier, and G—Gakona Glacier. See Fig. 2 for location.

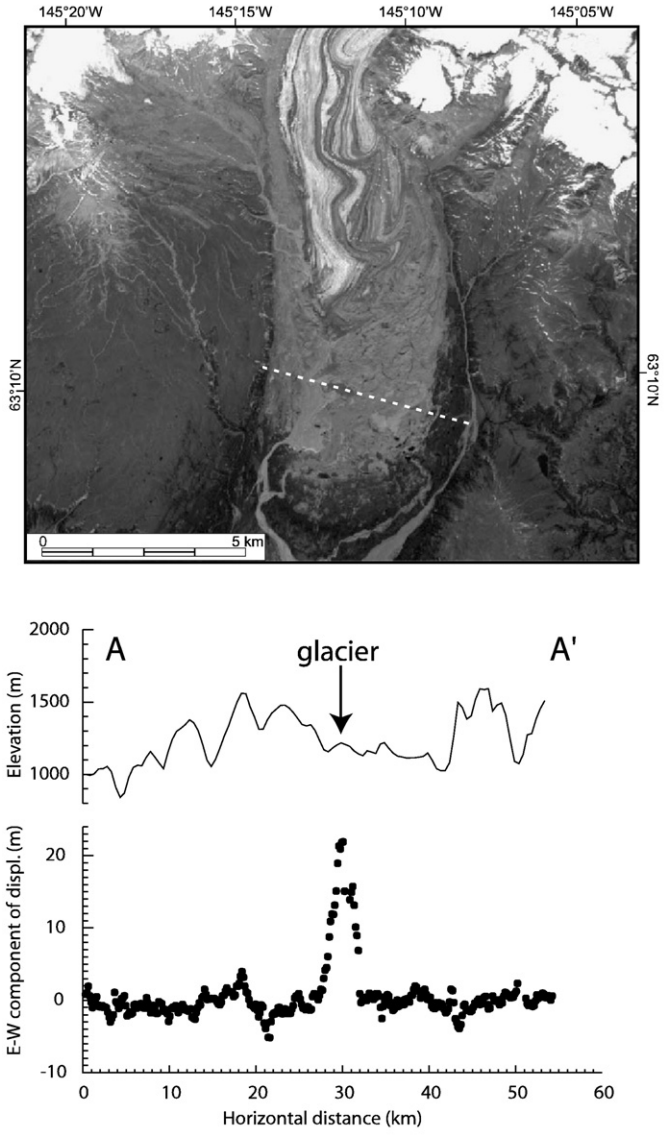

Fig. 9. (A) SPOT 4 image of the southeast flowing Gakona glacier. White dotted line shows location of elevation and fault parallel displacement values at distances 27–32 km's along the profiles shown in Fig. 9. See Fig. 8 for location. (B) Co-located profiles of elevation and the fault parallel horizontal displacement. In general, the displacement values hover around zero, but note the positive spike near 30 km. These values coincide with the Gakona glacier, and maximum displacement values occur in the center of the glacier, with values approaching zero near the glacier margins. See Fig. 8 for profile location.

above. To test for the potential effect of residual topography in the displacement maps, we plot the east–west component of the surface displacement and elevation along co-located NW–SE trending profiles (A–A′ in Fig. 9). There is no obvious correlation between the elevation and surface displacement, indicating that most photogrammetric parallax effects were successfully removed in the data processing. This conclusion is consistent with the data variance in the east–west displacement which is approximately 1.5 m (Fig. 9). Locally however, the displacement field yields anomalous values clearly observed in Fig. 9 that is due to the mobility or the high reflectance of the ice and snow cover, which we describe in the following section.

7. Effects of snow cover and glacier motion

For this study the SPOT images show a similar distribution of snow cover and glaciers at higher elevations in the northern part of both images (Fig. 7). Locally, glaciers flow along, and to the north and south of the Denali fault (e.g., the Canwell and Gakona glaciers). We emphasize the snow cover posed a significant challenge in the data processing, because the instrument becomes saturated as the snow and ice possess high reflectance; as a result, significant correlation is lost (Fig. 8). Locally however, snow cover is fortunately absent in the vicinity of the Denali fault, and also isolated patches of exposed bedrock, alluvial surfaces, and moraines occur to the north and south of the fault as well. The southern regions of the SPOT images are relatively devoid of snow cover.

An example of clear spurious displacements associated with ice flow is shown in Fig. 9, where between km 27 and 32 along profile A–A′ there is a large positive spike of approximately 23 m in the east–west component of the displacement map (Fig. 9). The large displacement values coincide with the toe of the Gakona glacier with peak displacement values in the center of the glacier (Fig. 9). As the glacier margins are approached the displacement values tend toward zero values, which is consistent with southeastward glacier flow (Fig. 9). The north–south component of the surface displacement field along the same co-located profile indicates a maximum southward displacement of ~8 m at km 30 consistent with southeast flow of the Gakona glacier at this location. Other clear examples of glacier flow are indicated in the horizontal displacement maps in Fig. 8, and include the Johnson, West Fork, and Chistochina glaciers.

8. Isolation and estimation of co-seismic displacements

Because we are interested in isolating the co-seismic displacement of the Denali 2002 earthquake, we designed a method to identify bias due to glacier flow by proceeding as follows. We first obtained SPOT imagery that covers a time period preceding the 2002 Denali earthquake (1999–2002). Next, we performed the sub-pixel correlation technique as described in Section 6 to obtain the horizontal offsets. We then assume that any horizontal offset larger than 3 m or having a low SNR is either related to glacial motion, or is decorrelated, and that area was masked. We then apply this mask to the sub-pixel correlation results using the image pair with the time span that includes the 2002 Denali earthquake. This approach effectively removes the majority of measured displacements due to glacial motion and isolates the tectonic signal of the 2002 Denali earthquake. Assuming that the entire glacial signal is removed, only the tectonic signal should remain. Field measurements indicate that the 2002 Denali earthquake is dominated by strike–slip motion and we project the north–south/east–west displacement field into fault parallel displacement. Fig. 10 is the sub-pixel correlation results after applying the masking routine. In general, the correlation map corrected for glacier motion shows a discontinuity oriented with the N75°W strike of the Denali fault. It is also worth noting that displacements do not exceed 10 m after the masking technique is applied. In general the displacement field shows positive values on the north side of the fault, and negative values on the south side, consistent with dextral motion along the Denali fault (Fig. 10).

A source of uncertainty in estimating the co-seismic displacement is related to the noise in the correlation maps, and any spatial variations in the ground displacement. In displacement profiles oriented perpendicular to the trace of the Denali fault such as those shown in Fig. 10B and C, all data points within a given box are projected onto the displacement profiles. This approach emphasizes the spatial dispersion of the displacement data which contributes to the uncertainty in estimating the co-seismic displacement. An additional source of uncertainty in the correlation maps are associated with errors in the DEM that can be sourced to regions with high slope and can be azimuth dependent. Fig. 10D is a plot of the RMS error calculated from the DEM and the E–W horizontal offsets. In the absence of ancillary data we rely on the fact that the offset values we obtain are more tightly clustered near low RMS values. We perform a

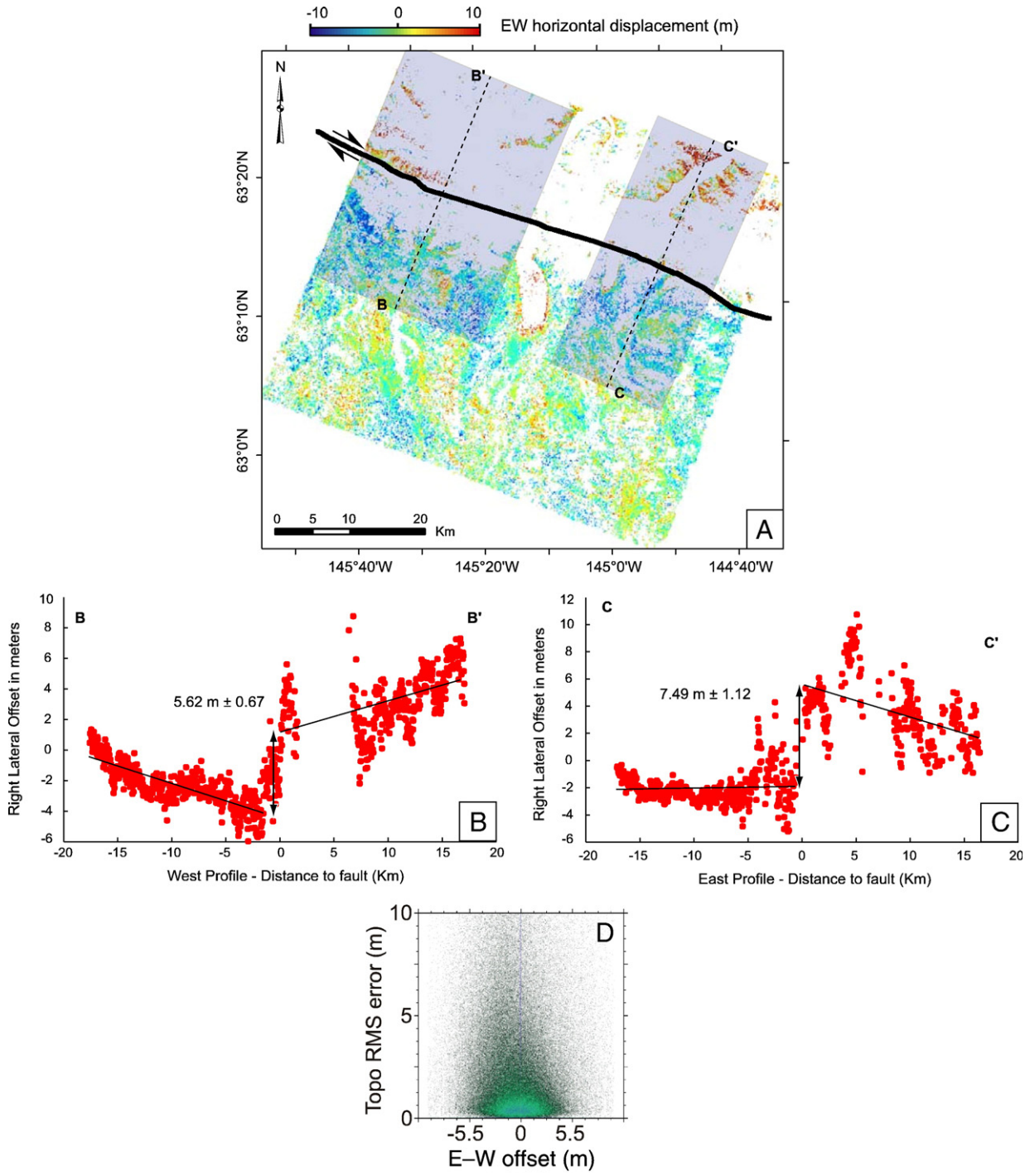

Fig. 10. (A) Map of the horizontal offset surface displacement field with effects of decorrelation and glacier flow removed using the masking process described in Section 4. Masked regions appear in white. Note that maximum displacements do not exceed 10 m. We use the convention where eastward displacements are positive. Arrows indicate location of the Denali fault. See Fig. 2 for location. (B–C) Plots of fault parallel displacement after masking was applied. Data are projected from data swaths emphasizing the spatial variability in ground displacement. See Fig. 10A for profile locations. (D) Scatter plot of RMS error from the NED DEM and E–W displacement. See text for a discussion.

linear least-squares fit to the displacement profiles to estimate the mean slip across the fault and a 2 sigma uncertainty is estimated to the least-squares fit.

In Fig. 10B and C, the profiles B–B′ and C–C′ are oriented perpendicular to the trace of the Denali fault and are separated by approximately 30 km to investigate any along strike variation in the horizontal displacement field. Profile B–B′ indicates negative values on the south side of the Denali fault that increase southward to zero values near −18 km along the profile. An abrupt deformation signal of 5.6±0.67 m is concentrated on the Denali fault over a 2–3 km wide zone. The width of the deformation zone estimated from the displacement profiles likely reflects the fact that the Denali fault is not perfectly straight, but locally exhibits variations in fault strike, again emphasizing the spatial dispersion in the displacement field as the data are projected onto the profile. North of the fault zone, the mean displacement values increase from 0–4 m. It is difficult to isolate the exact cause of the apparent displacement north of km 10 along the profile. However, we note that the SPOT correlation offsets are accurate when looking at relative displacements, but absolute displacements may be corrupted by residuals from the satellite

attitudes, which can be hard to correct for. The long wavelength artifacts observed in the profiles may be attributed to uncorrected variations of the pitch and roll of the satellite. We are aware of these limitations, which is why we limit our analysis to the measurement at the Denali fault. The abrupt changes we observe in the correlation maps and in the displacement profiles at the Denali fault are unlikely to result from errors in the satellite attitude residuals. Therefore, the horizontal offset measurements we obtain should not be biased by any long wavelength artifacts.

Profile C–C′ shows the fault parallel displacement, which displays a slightly lower displacement gradient in comparison to the previous profile. The displacement field shows that negative values increase southward to zero displacement near −17 km, with an abrupt displacement signal concentrated on the Denali fault (Fig. 10C). The displacement here, is apparently higher than that observed for profile B–B′ with a value of 7.5±1.12 m with the displacement approaching zero near 17 km on the profile.

The observations in the displacement profiles in Fig. 10B and C can be well explained by a vertical strike–slip fault that exhibits an along-strike variation in dextral co-seismic slip, with 7.5±1.12 m in the east that is apparently more localized, which decreases to 5.6±0.67 m in the west (Fig. 10). The surface slip estimates we obtain are in general consistent with previous field observations (although there are complications associated with the field measurements, as discussed in Haeussler et al. (2004) and geodetically determined estimates of co-seismic fault slip (Hreinsdottir et al., 2003; Dreger et al., 2004; Elliott et al., 2007).

9. Implications for the mechanics of fault rupture and secondary off-fault deformation

The 2002 event, as revealed by previous field measurements (Eberhart-Phillips et al., 2003; Haeussler et al., 2004) and observations of seismic and geodetic data (Hreinsdottir et al., 2003; Dreger et al., 2004; Elliott et al., 2007) suggests that at the scale of approximately 10 km, the highly variable slip observed at the surface also extends to depth. In comparison, this study shows that glacial ice in addition to being a source of noise in the sub-pixel correlation can also be an exceptional strain marker for documenting distributed deformation, that otherwise may not be as easily seen. The aerial photographs in Section 5 show that the zone of distributed strain may have a finite width of up to a few hundred meters that extends off the main rupture trace. In particular, we observe a clear example of distributed strain over a zone of finite width near the western margin of the Chistochina glacier (Fig. 6). It is worth noting that in the case of the Denali event, the collective variability observed in magnitude of off-fault deformation, magnitude of slip, and deflection of the rupture trace, occurs in some cases at material boundaries between glaciers, alluvium, and tundra (e.g., Fig. 6). This observation suggests that a significant portion of co-seismic slip may in some cases escape detection by conventional field measurements alone, and that sub-pixel correlation of optical imagery can be a particularly useful tool.

Using the sub-pixel correlation technique, we have determined that the average mean slip for the Denali 2002 event is closer to the maximum offsets measured in the field, rather than their mean values. This behavior is also observed for the Hector Mine and Landers earthquakes, as shown in LePrince et al. (2007), and Michel et al. (1999), which were found to correspond to regions of distributed off-fault deformation, that were previously inferred to be a seismic "slip-gap" (at least for the Lander's event) (Spotila and Sieh, 1995). If this inference is correct, an alternative possibility arises for interpreting the along-strike variability in fault slip; that is, the slip variability observed in the field may actually reflect lateral variations in the mechanical response of near-surface layers to the dynamics of earthquake rupture (Poliakov et al., 2002). Poliakov et al. (2002) demonstrated for strike–slip events that the magnitude of secondary off-fault deformation, and the generation of bends in the rupture geometry, depends in part on variations in the rupture velocity of the material, and also the regional stress field to a degree. We suggest that the lower values of fault slip reflects the variability of material properties near the surface, and that higher values of co-seismic slip reflects the deeper and true amount of slip related to the Denali 2002 earthquake.

10. Regional tectonic implications for westward decrease in fault slip for the 2002 Denali earthquake

SPOT horizontal offsets generated by the sub-pixel correlation technique are able to reveal rupture characteristics related to the November 2002 Denali earthquake. The results indicate that 7.5 m of slip occurred in the east and decreased to 5.6 m in the west between longitudes 144°52′W and 145°45′W, respectively. Similarly, previous field and geodetic observations also indicate an along-strike decrease in dextral fault slip from east to west. The co-seismic behavior of the great 2002 Denali earthquake raises the question, does the first-order asymmetric slip distribution represent the long-term behavior of the Denali fault, and if so, what are the implications for the long-term behavior of the Denali fault system and subsequent growth of the Alaska Range? The tectonic geomorphology along the northern range front of the Alaska Range described in Section 2 suggests that regional slip partitioning between the right slip Denali fault and east-trending contractional structures near the apex and further to the west contribute to the asymmetric geometry of the Alaska Range.

It has been postulated that the Denali fault accommodates vertical axis counterclockwise rotation of south Alaska (Lahr and Plafker, 1980; Fletcher and Freymueller, 2000; Fletcher, 2002). An alternative possibility is a kinematic model that incorporates the northwestward translation of southern Alaska and slip partitioning between the arcuate Denali strike–slip fault and neighboring folds and thrust faults, as first suggested by Stout and Chase (1980) and later modeled by Bird (1996). In a finite element model of Alaska (Bird, 1996), the preferred result indicates a slip rate of 13 mm/yr on the Shakwak segment of the Denali fault near 145°W, which decreases to 6 mm/yr near longitude 150°W. Additionally in that model (Bird, 1996; Stout and Chase, 1980), near and to the west of 150°W, crustal thickening is accommodated to the south of the Denali fault on the southeast-directed Broxson Gulch and Pass Creek thrust faults, which occur in the general vicinity of, and exhibit similar fault geometry and kinematics as the Susitna Glacier thrust fault. The thrust faults in the best model have slip rates between 3 and 6 mm/yr. A limitation of the regional model is that the slip rates are biased by the number of faults present, and a realistic treatment of the Alaska Range is that locally, more active thrusts are probably present, which would result in lower slip rates for individual thrust faults. A more recent study on the post-glacial slip-rate of the Denali fault also found that the dextral slip rate decreases to the west by nearly a factor of two (Meriaux et al., 2008). As a result, the decrease in dextral slip rate is accommodated by an increase in shortening rate perpendicular to the Denali fault as Mt McKinley is approached from the east (Meriaux et al., 2008). In a GPS study conducted prior to the Denali earthquake, Fletcher (2002) found geodetic evidence suggesting that several active structures interpreted to be right-slip faults are located to the north of the Denali and most likely correspond to the Hines Creek fault. Collectively, it appears that the long-term behavior between the Denali fault and the central Alaska Range (Eisbacher, 1976; Hickman et al., 1977; Jones et al., 1982; Plafker et al., 1989; Nokelberg et al., 1992; Plafker and Berg, 1994; Bird, 1996) is strikingly consistent with the complex rupture of the December 2002 event, and suggests the Denali fault plays a critical role in crustal thickening along its central and western segments. This prediction may be tested by future neotectonic studies of the Alaska Range.

11. Conclusions

We use SPOT image pairs to determine horizontal offsets associated with the M 7.9 November 2002 Denali earthquake in the vicinity of Slate Creek, Alaska. We identify horizontal motions that are related to glacier motions, which exceed the co-seismic displacements. To remove the effects of glacial motion we use a masking procedure to isolate the tectonic signal. The SPOT horizontal offsets are consistent with previous field and geodetic studies with a displacement field that shows a signal that can be well-explained by an along-strike variation in dextral shear. Approximately 7.5 m of dextral shear is documented in the east near 144° 52′W. Dextral slip decreases to 5–6 m to the west near 145° 45′W. Field observations and aerial photographs also characterize the detailed geometry of the surface rupture. Our observations imply that shear localization is more likely where fault strands are linear and continuous, whereas distributed off-fault deformation is likely to occur either at fault bends and step-overs, or material boundaries (e.g., contacts between soft glacial sediments, ice, and rock). If the November 2002 earthquake reflects the long-term behavior of the Denali fault, it implies a westward decrease in the faults long-term slip rate. A possible mechanism to accommodate the westward decreasing slip on the Denali fault is to transfer slip to adjacent east-trending contractional structures in the west. South-directed slip on the Susitna Glacier thrust fault and the geomorphology of the Northern Foothills of the Alaska Range, which is consistent with an active north directed thrust system suggests that this is a possibility. Future field studies are necessary to test this hypothesis.

Acknowledgements

M. Taylor thanks the Tectonics observatory at Caltech for partial support during this research. We are grateful to Aron Meltzner for careful scanning of the aerial photographs. This study has benefited from discussions with David Schwartz, Peter Haeussler, An Yin, Gilles Peltzer, Aron Meltzner, Francois Ayoub, Alex Robinson, Doug Walker, and Anne Sophie-Meriaux, which were extremely helpful in organizing our thoughts. We appreciate the constructive comments made by two anonymous reviewers that helped to clarify several points.

References

Bemis, S., 2004. Neotectonic Framework of the North-Central Alaska Range Foothills, MS. University of Alaska, Fairbanks.
Bird, P., 1996. Computer simulations of Alaskan neotectonics. Tectonics 15, 225–256.
Cole, R., Ridgeway, K., Layer, P., Drake, J., 1999. Kinematics of basin development during the transition from terrane accretion to strike–slip tectonics, Late Cretaceous Early Tertiary Cantwell Formation, south central Alaska. Tectonics 18, 1224–1244.
Csejtey, B., Mullen, M., Cox, D., Stricker, G., 1992. Geology and Geochronology of the Healy Quadrangle, South-Central Alaska:, U.S. Geological Survey Miscellaneous Investigation Map I-1961, Scale 1:250,000.
Dreger, D., Oglesby, D., Harris, R., Ratchkovski, N., 2004. Kinematic and dynamic rupture models of the November 3, 2002 Mw7.9 Denali, Alaska, earthquake. Geophys. Res. Lett. 31. doi:10.1029/2003GL018333.
Eberhart-Phillips, D., Sieh, K., Rubin, C., 2003. The 2002 Denali Fault earthquake, Alaska. Science 300, 1113–1118.
Eisbacher, G., 1976. Sedimentology of the Dezadeash flysch and its implications for strike–slip faulting along the Denali fault, Yukon Territory and Alaska. Can. J. Earth Sci. 13, 1495–1513.
Elliott, J., Freymueller, J., Rabus, B., 2007. Coseismic deformation of the 2002 Denali fault earthquake: contributions from synthetic aperture radar range offsets. J. Geophys. Res. 112. doi:10.1029/2006JB004428.
Fialko, Y., 2004. Probing the mechanical properties of seismically active crust with space geodesy. J. Geophys. Res. B, Solid Earth Planets 109. doi:10.1029/2003JB002756.
Fletcher, H., 2002. Crustal Deformation in Alaska Measured using the Global Positioning System, PhD. University of Alaska, Fairbanks.
Fletcher, H., Freymueller, J., 2000. Using GPS to unravel the tectonics of interior Alaska. Eos 81, 1126.
Haeussler, P., Schwartz, D., Dawson, T., Stenner, H., Lienkaemper, J., Sherrod, B., Cinti, F., Montone, P., Craw, P., Crone, A., Personius, S., 2004. Surface rupture and slip distribution of the Denali and Totschunda Faults in the 3 November 2002 M 7.9 Earthquake, Alaska. Bull. Seismol. Soc. Am. 94, S23.
Hickman, R., Craddock, C., Sherwood, K., 1977. Structural geology of the Nenana River segment of the Denali fault system, central Alaska Range. Geol. Soc. Amer. Bull. 88, 1217–1230.
Hreinsdottir, S., Freymueller, J.T., Burgmann, R., Mitchell, J., 2006. Coseismic deformation of the 2002 Denali Fault earthquake: insights from GPS measurements. J. Geophys. Res.-Solid Earth 111. doi:10.1029/2005JB003676.
Hreinsdottir, S., Freymueller, J., Fletcher, H., Larsen, C., Burgmann, R., 2003. Coseismic slip distribution of the 2002 Mw7.9 Denali fault earthquake, Alaska, determined from GPS measurements. Geophys. Res. Lett. 30, 1670. doi:1610.1029/2003GL017447.
Jones, D., Siberling, N., Gilbert, W., Coney, P., 1982. Character, distribution, and tectonic significance of accretionary terranes in the central Alaska Range. J. Geophys. Res. 87, 3709–3717.
Lahr, J., Plafker, G., 1980. Holocene Pacific-North American plate interaction in southern Alaska: implications for the Yakataga seismic gap. Geology 8, 483–486.
LePrince, S., Barbot, S., Ayoub, F., Avouac, J.P., 2007. Automatic and precise orthorectification, coregistration, and subpixel correlation of satellite images, application to ground deformation measurements. IEEE Trans. Geosci. Remote Sens. 45, 1529–1558.
McGill, S., Rubin, C., 1999. Surficial slip distribution on the central Emerson fault during the June 28, 1992, Landers earthquake. J. Geophys. Res. 104, 4811–4834.
Meriaux, A.S., Sieh, K., Finkel, R., Rubin, C., Taylor, M., Meltzer, A.S., Ryerson, F., 2008. Kinematic behavior of southern Alaska constrained by westward-decreasing post-glacial slip-rates on the Denali fault, Alaska. J. Geophys. Res. in revision.
Michel, R., Avouac, J.P., Taboury, J., 1999. Measuring near field coseismic displacements from SAR images. Geophys. Res. Lett. 26, 3017–3020.
Nokelberg, W., Aleinikoff, J., Dutro, J., Lanphere, M.A., Silberling, N., Silva, S., Smith, T., Turner, D., 1992. Map, Tables, and Summary of Fossil and Isotopic Age Data, Mount Hayes Quadrangle, Eastern Alaska Range, Alaska, U.S. Geological Survey Miscellaneous Field Studies Map 1996-D, scale 1:250,000.
Nokelberg, W., Jones, D., Siberling, N., 1985. Origin and tectoonic evolution of the Maclaren and Wrangellia terranes, eastern Alaska range, Alaska. Geol. Soc. Amer. Bull. 96, 1251–1270.
Pewe, T., Wahrhaftig, C., Weber, F., 1966. Geologic Map of the Fairbanks Quadrangle, Alaska, U.S. Geological Survey Miscellaneous Investigation Map I-0455, scale 1:250,000.
Plafker, G., Berg, H. (Eds.), 1994. An Overview of the Geology and Tectonic Evolution of Alaska. The Geological Society of America, Boulder, Co. 989–1021 pp.
Plafker, G., Nokelberg, W., Lull, J., 1989. Bedrock geology and tectonic evolution of the Wrangellia, Peninsular, and Chugach terranes along the trans Alaska crustal transect in the northern Chugach Mountains and southern Copper River basin. J. Geophys. Res. 94, 4255–4295.
Poliakov, A., Dmowska, R., Rice, J., 2002. Dynamic shear rupture interactions with fault bends and off-axis secondary faulting. J. Geophys. Res. B, Solid Earth Planets 107. doi:10.1029/2001JB000572.
Ridgeway, K., Trop, J., Nokelberg, W., Davidson, C., Eastham, K., 2002. Mesozoic and Cenozoic tectonics of the eastern and central Alaska Range: progressive basin development and deformation in a suture zone. Geol. Soc. Amer. Bull. 114, 1480–1504.
Simons, M., Fialko, Y., Rivera, L., 2002. Coseismic deformation from the 1999 Mw 7.1 Hector Mine, California, earthquake as inferred from InSAR and GPS observations. Bull. Seismol. Soc. Am. 92, 1390–1402.
Spotila, J., Sieh, K., 1995. Geologic investigations of a "slip gap" in the surficial ruptures of the 1992 Landers earthquake, Southern California. J. Geophys. Res. B, Solid Earth Planets 100, 543–559.
Stout, J., Chase, C., 1980. Plate kinematics of the Denali fault system. Can. J. Earth Sci. 17, 1527–1537.
Van Puymbroeck, N., Michel, R., Binet, R., Avouac, J.P., Taboury, J., 2000. Measuring earthquakes from optical satellite images. Appl. Opt. 39, 3486–3494.
Wahrhaftig, C., 1970a. Geologic Map of the Fairbanks A-2 Quadrangle, Alaska, Geological Survey Geologic Quadrangle Map GQ-808, Scale 1:63 360.
Wahrhaftig, C., 1970b. Geologic Map of the Fairbanks A-3 Quadrangle, Alaska, U.S. Geological Survey Geologic Quadrangle Map GQ-809, Scale 1:63 360.
Wahrhaftig, C., 1970c. Geologic Map of the Fairbanks A-4 Quadrangle, Alaska, U.S. Geological Survey Geologic Quadrangle Map GQ-810, Scale 1:63 360.
Wahrhaftig, C., 1970d. Geologic Map of the Fairbanks A-5 Quadrangle, Alaska:, U.S. Geological Survey Geologic Quadrangle Map GQ-811, Scale 1:63 360.
Wahrhaftig, C., 1970e. Geologic Map of the Healy D-2 Quadrangle, Alaska, U.S. Geological Survey Geologic Quadrangle Map GQ-804, Scale 1:63 360.
Wahrhaftig, C., 1970f. Geologic Map of the Healy D-3 Quadrangle, Alaska, U.S. Geological Survey Geologic Quadrangle Map GQ-805, Scale 1:63 360.
Wahrhaftig, C., 1970g. Geologic map of the Healy D-4 quadrangle, Alaska. Geologic Map of the Healy D-4 Quadrangle, Alaska.
Wahrhaftig, C., 1970h. Geologic Map of the Healy D-5 Quadrangle, Alaska: U.S. Geological Survey Geologic Quadrangle Map GQ-807, Scale 1:63 360.
Wahrhaftig, C., 1958. Quaternary geology of the Nenana River valley and adjacent parts of the Alaska Range. U.S. Geol. Surv. Prof. Pap. 293-A, 1–68.
Wahrhaftig, C., 1968. Schists of the Alaska Range. U.S. Geol. Surv. Bull. 1254-E, E1–E22.
Wahrhaftig, C. (Ed.), 1987. The Cenozoic section at Suntrana, Alaska. Geological Society of America. 445–450 pp.
Wald, D., Heaton, T., 1994. Spatial and temporal distribution of slip for the 1992 Landers, California, earthquake. Bull. Seismol. Soc. Am. 84, 668–691.
Wahrhaftig, C., Turner, D., Weber, F., Smith, T., 1975. Nature and timing of movement on the Hines Creek strand of the Denali fault system, Alaska. Geology 3, 463–466.
Wahrhaftig, C., Wolfe, J.A., Leopold, E.B., Lanphere, M.A., 1969. The Coal-Bearing Group in the Nenana coal field, Alaska. U.S. Geol. Surv. Bull. 1274-D, 1–30.